Transition between Icosahedral and Cuboctahedral Nanoclusters of Lead

C. M. Wei

Institute of Atomic and Molecular Sciences, Academia Sinica, Taipei 106, Taiwan, Republic of China, and Institute of Physics, Academia Sinica, Nankang, Taipei 115, Taiwan, Republic of China

C. Cheng*

Department of Physics, National Cheng Kung University, Tainan 701, Taiwan, Republic of China

C. M. Chang

Department of Physics, National Dong Hwa University, Hualien 974, Taiwan, Republic of China

Received: June 26, 2006; In Final Form: September 19, 2006

We have used ab initio methods to study the possible transition between icosahedral (ico) and cuboctahedral (fcc) structures in lead nanoclusters of sizes up to 309 atoms. Spontaneous fcc-to-ico transition in Pb_{13} was observed in the ab initio molecular dynamics (MD) simulations at various temperatures. The transition path can be described predominantly by an angular variable *s*, which can, generally be applied to the similar transitions in clusters of larger sizes and was observed to follow the Mackay model. We have calculated the two-dimensional energy surface that describes the transition in Pb_{13} and found a barrierless fcc-to-ico transition path, which is consistent with the observed spontaneous transition in the ab initio MD simulations. The atomic displacements in the transition were identified as one of the vibrational eigenmodes of these two Pb_{13} clusters. For clusters of larger sizes (Pb_n, where $n = 55$, 147, and 309), the possible transitions following similar paths were determined not to be barrierless and the sizes of the barriers were determined by the ab initio elastic band method.

Introduction

Nanoparticles can have a structure that is prohibited in the crystallographic translational-symmetry rules (e.g., the icosahedra (ico) and decahedra (deca) with noncrystalline 5-fold symmetry). Nanoparticles of elements that have a cuboctahedral (fcc) bulk structure have been observed to have structures with 5-fold symmetry; the most-studied ones include some metallic and rare-gas clusters.[1] As the growth of clusters proceeds beyond a crossover point, a structural transition to the crystalline structures is expected to occur. Experimentally, it has been observed that the structural transitions in clusters are dependent on the sizes of the nanoparticles, as well as the temperature,[2] which demonstrated that the stable structures and transition barriers between metastable structures are both size-dependent. Concerning studies for the transition between crystalline- and noncrystalline-symmetry structures in clusters, previous theoretical studies primarily use classical molecular dynamics (MD) simulations with various empirical interatomic potentials, and the transition is well-known to be dependent on the potentials used.[3,4] Mackay has proposed a transition model between the 5-fold-symmetry ico and the crystalline structure of fcc cuboctahedra,[5] which, to our knowledge, has never been investigated using state-of-the-art ab initio methods. The ico ↔ fcc transition can be a crucial process near the cross-over point from clusters to the crystalline structure.

In this article, we first show that the Mackay model for the ico ↔ fcc transition in clusters can be described predominantly by an angular variable *s*. Works with similar recognition has existed for rare gas clusters with effective potentials.[6] We then demonstrate, using first-principles MD simulations, that a spontaneous fcc-to-ico transition can be observed in Pb_{13} and the transition indeed follows the Mackay path. The Pb_{13} systems were studied further by the corresponding two-dimensional (2D) energy surface in the transition, as well as the connection between the normal modes of the clusters and the transition path. Transitions through similar paths were applied to Pb_n of larger sizes (where $n = 55$, 147, 309) by the ab initio elastic band method[7] and were all determined to possess finite barriers.

Theory and Procedure

The Mackay model for the ico ↔ fcc transition in 13-atom and 55-atom clusters are schematically illustrated in Figures 1a and 1b, respectively. The left-most panels show the ico structures with I_h symmetry, and the right-most panels are the fcc structures with O_h symmetry. Because these structures are highly symmetrical, all atoms except the center one can be separated into groups of atoms that are connected by symmetry operations. Therefore, the original complexity in the structural transition can be greatly reduced, because of the high-symmetry constraints. In fact, by keeping the cluster within the T_h symmetry (the common subgroup of I_h and O_h), the cluster can easily transform between the icosahedra (I_h symmetry) and the fcc (O_h symmetry) structures (see Figure 1). Specifically, for the 13-atoms cluster, it can be viewed as one atom moving in a 2D symmetry plane and only two variables are needed to describe the cluster. The first variable, *r*, is the interatomic distance of the outer atoms to the center atom. The second variable, *s*, describes the angular portion of the outer atom in the 2D plane.

$$\Theta = \tan^{-1}\sqrt{\frac{2-s}{2+s}}$$

It is easy to verify that, if $s = \pm\sqrt{0.8}$, then the structure is ico;

10.1021/jp063982o CCC: $33.50
Published on Web 11/10/2006

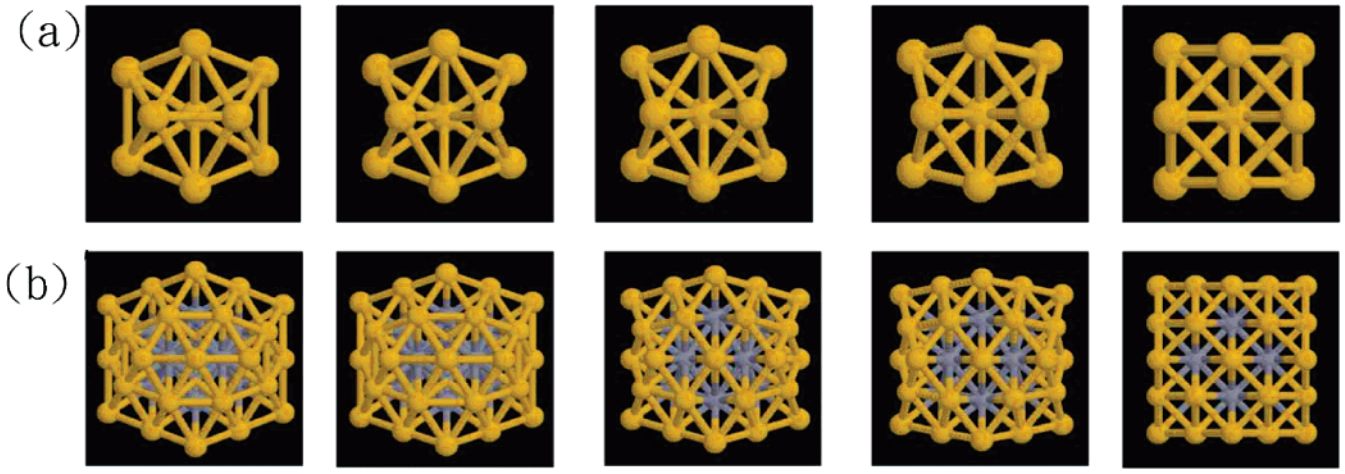

Figure 1. Structural transition between icosahedral (ico; see the left-most panel) and cuoctahedreal (fcc; see the right-most panel) in (a) 13-atom and (b) 55-atom clusters, following the change of variable *s*, as described in the text.

if $s = 0$, the structure is fcc. When *s* changes from $\pm\sqrt{0.8}$ to 0, the cluster undergoes the ico-to-fcc transition, as shown in Figure 1a. For larger clusters, if all the atoms in the clusters are kept at their fractional positions defined by the center atom and the other 12 vertex atoms, then the same variables *r* and *s* can be used to describe the ico ↔ fcc transition of larger clusters. From the aforementioned analysis, indeed, the Mackay model for the ico ↔ fcc transition can be described using only two variables.

The previously given description of the ico ↔ fcc transition can be observed in Pb_{13} by ab initio MD simulations. All electronic calculations in this study are based on the density functional theory (DFT)[8] with the proposed generalized gradient approximation (GGA) by Perdew, Burke, and Ernzerhof[9] for the nonlocal correction to a purely local treatment of the exchange-correlation potential and energy. The single-particle Kohn−Sham equations[10] are solved using the plane-wave-based Vienna ab initio simulation program (VASP) developed at the Institut für Material Physik of the Universität Wien in Austria.[11] The interactions between the ions and valence electrons are described by the projector augmented-wave (PAW) method[12] in the implementation of Kresse and Joubert.[13] The numbers of treated valence electrons are four and three for Pb and Al atoms, respectively; we shall discuss the Al clusters later in this paper. The energy cutoffs for the plane-wave basis are 100 and 241 eV for the Pb and Al systems, respectively. The calculated structural data for Pb—e.g., the dimer bond length (2.939 Å) and the lattice constant of the bulk (5.026 Å)—compare well with the experimental values (2.932 Å[14] and 4.95 Å). The binding energy of the dimer (1.24 eV) and the cohesive energy of the bulk (2.99 eV) deviate more from the experimental values (0.86 eV[15] and 2.03 eV). These departures are frequently observed in the LDA/GGA calculations for cases that involve bond breaking. A recent relativistic all-electrons study showed that for Pb dimer the deviation was mainly from the spin−orbit coupling.[16] Because the systems that we studied consisted of at least 13 Pb atoms and all the investigations concern structural changes for the clusters of the same size, it is expected,[17] as many previous studies have demonstrated, that the nature of bonds does not change much in different structures for clusters of the same size and, therefore, the methods are likely to be applicable to the present study.

All clusters were simulated by them being placed in the center of cubic supercells that are large enough to neglect cluster−cluster interactions; i.e., a spacing of at least 10 Å, separated by a vacuum between the atoms of neighboring clusters, was used in the simulations. The supercells are at least 14 Å in length, and go up to 38 Å for Pb_{309}; thus, only one *k*-point at the gamma point was included in the integration of the Brillouin zone. Relaxation processes in optimizing static structures were accomplished by moving atoms to the positions at which all atomic forces were <0.02 eV/Å. The molecular dynamics of the system was simulated by the canonical Nosé dynamics[18] with a fictitious mass of 2 amu and at least 10 000 time steps with a step size of 1 fs.

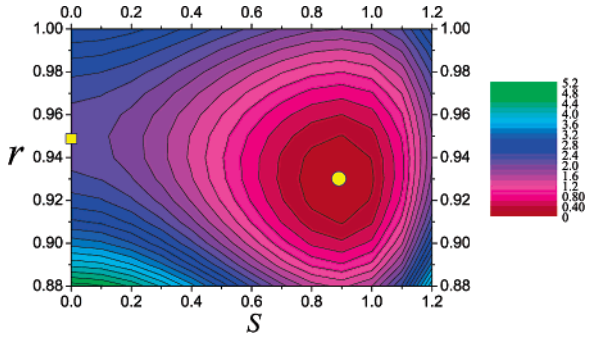

Figure 2. Calculated energy surface of Pb_{13} in the two-dimensional (2D) space of the variable *s* and the interatomic distance *r*. The spacing between the energy contours is 0.2 eV per cluster. The locations for the ico and fcc structures are designated by the circle and the square, respectively.

In the static calculations of Pb_{13}, the ico structure was determined to be more stable than the fcc structure by 2.08 eV (per cluster). Starting with the fcc structure of Pb_{13}, we performed a few ab initio MD simulations of the system at various temperatures. The initial configurations of the MD simulations were taken as the static fcc Pb_{13} plus the randomly set atomic velocities, according to the Maxwell−Boltzmann distribution at temperatures of 50, 100, 300, and 500 K. In all cases, the fcc-to-ico transition, which followed the previously discussed Mackay path, was observed in the beginning of the simulation and succeeded by thermal vibrations about the ico structure. The fact that the fcc-to-ico transition happens at the beginning of the MD simulations for all the temperatures we studied suggests a barrierless transition in Pb_{13}. To verify this point, the energy surface of Pb_{13} on the 2D space of the transition variable *s* and the interatomic distance *r* was calculated and the result presented in Figure 2. The electronic energy of a total of 169 structures on this 2D space were evaluated, i.e., 13 values of the variable *s* (ranging from 0.0 to 1.2) and 13 values for the interatomic distance *r* (ranging from 0.88 to 1.00) (given

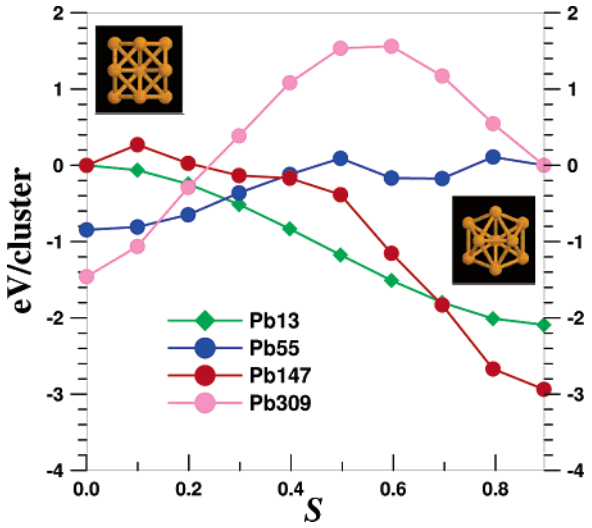

Figure 3. Energy curves obtained from the ab initio elastic band method for the ico ↔ fcc transition in Pb clusters, following the same transition path as those depicted in Figure 1. The energy of the higher-energy structure is taken as the zero energy.

in units of the nearest-neighbor distance in bulk Pb) were considered. The ico Pb_{13} is located at the bottom of the energy surface, whereas the fcc Pb_{13} is observed at a saddle point. According to this 2D energy surface, the fcc-to-ico transition in Pb_{13} is indeed barrierless, as implied in the MD simulation. The energy space of a 13-atom cluster, of course, consists of much more than two degrees of freedom. In fact, it consists of 33 degrees of freedom. However, we have used ab initio MD simulations to demonstrate that the fcc-to-ico transition in Pb_{13} does follow the two-variable transition path, although its 33-dimensional energy surface can, in principle, be very complicated.

It is expected that, when the transition state approaches either terminal structure, the atomic displacements should be able to be described by an eigenmode of vibration or a linear combination of eigenmodes of the terminal structures. We have calculated the vibrational frequencies of the ico and fcc Pb_{13} through the Hessian matrix, as provided in VASP. The atomic displacements of one of the vibrational eigenmodes of the ico and fcc Pb_{13} were determined to be identical to the proposed description of transition. The eigenfrequencies are 1.82 (real value) and 1.30 (imaginary value) THz for the ico and fcc Pb_{13}, respectively. The soft mode (imaginary frequency) corresponds to the negative curvature of the energy curve along the transition path at the fcc Pb_{13}, as shown in Figure 2. This is the only soft mode found in fcc Pb_{13}. The fact that all the vibrational frequencies obtained for the ico Pb_{13} are real indicates that ico Pb_{13} is a stable structure and, on the 2D energy surface, it is located at the bottom of a valley.

This description of ico ↔ fcc transition can generally be applied to the clusters of larger sizes, as discussed previously (for example, see Figure 1b for the 55-atom cluster). Because the fcc-to-ico transition in Pb_{13} is barrierless, it will be interesting to know the sizes of the barriers for the larger Pb clusters. The results of fcc and ico Pb_n clusters (for $n = 55$, 147, and 309) and their fcc ↔ ico transition energy curves, including $n = 55$, 147, and 309, are plotted in Figure 3. The energy curves for the ico ↔ fcc transition were obtained from the elastic band method, with eight configurations between the terminal structures of ico and fcc. The initial atomic structures for these eight configurations were constructed from the structures of the corresponding variable *s*, as well as the linear scaling of the bond lengths between the ico and fcc structures. Note that the barriers described here are those from the higher-energy state to the lower-energy state (i.e., it is the barrier of the ico-to-fcc transition in Pb_{55} and Pb_{309} but the fcc-to-ico transition in Pb_{13} and Pb_{147}). After a closed-shell structure (e.g., ico of Pb_{13}) is formed, a larger closed-shell structure (e.g., ico of Pb_{55}) can be easily grown by adding atoms to the smaller structure, although ico is less stable than fcc in Pb_{55}. The barrier that then needs to be overcome for the transition from ico to the more-stable fcc form in Pb_{55} is the barrier that we discuss here. According to the calculations, the energy barrier increases as the size of the cluster increases: i.e., ~0.1, 0.3, and 1.5 eV for the transitions in Pb_{55}, Pb_{147}, and Pb_{309}, respectively. One may have a tendency to consider the energy barriers in terms of energy per atom, the values of which are all considerably smaller than the classical room-temperature thermal energy. However, it should be recognized that the transition path that we discuss here corresponds to an all-together movement, i.e., a particular displacing manner of the entire cluster that cannot be achieved by simply adding the random displacement of the individual atoms in the clusters. Therefore, transitions generally are not available at moderate temperature, as demonstrated for Au clusters experimentally.[2]

From Figure 3, one also notices that the relative stability of ico and fcc structures actually oscillates as the cluster size increases. One observation that is worthy of mention here is the fact that this surprising oscillating behavior is quite different from the results obtained by Lennard-Jones clusters,[19] where the energy of ico is always lower than that of fcc for clusters of sizes up to 147 atoms. It has also been demonstrated that different potentials could lead to different relative stabilities.[20] This fact suggests that ab initio DFT should be used to take the many-electron effects into account, in regard to studying nano-sized clusters. However, also note that the comparison here is only for the two structures studied here (i.e., fcc and ico). Another high-symmetry cluster that is frequently considered in the studies of clusters is the deca structure. Our calculations show that the deca structure is the lowest energy state of the three high-symmetry structures of ico, fcc, and deca in Pb_{55}, the highest in Pb_{309}, and in the middle of ico and fcc in Pb_{13} and Pb_{147}. The origin of the oscillating stability between the ico and fcc structures in Pb clusters, as well as comparison with the behaviors of other metallic nanoclusters, are presently under investigation and the results will be published soon.

In the case where the symmetry of the cluster is broken, the description of the transition model requires more than two variables, because the values of *r* and *s* are no longer identical for all the atoms (except the center one) in the cluster. Al_{13} is well-known to have a distorted ico structure.[21] The fcc Al_{13} is higher in electronic energy than the distorted ico Al_{13} by 0.9 eV (per cluster) in our calculations and the distorted ico is 0.1 eV lower in energy than the undistorted one. We have performed ab initio MD calculations for Al_{13}, similar to what we did for Pb_{13}, and the transition was also observed to approximately follow the variable *s*. Therefore, the path for the ico ↔ fcc transition is not strictly confined to the transition between the symmetry group of the ico and fcc. For clusters of sizes larger than 13 atoms, the number of variables are more than two, even when the symmetry of the cluster is not broken (e.g. the different interatomic distances for atoms in different shells). In these systems, the transition can still possibly follow the Mackay path. We have applied the embedded-atom-method MD to the Pd_{309}[22] clusters, and the fcc-to-ico transition through the Mackay path was also observed. Note that, in the embedded-

atom method, the ico structure has a lower energy than the fcc structure in Pd_{309}.

Conclusion

In conclusion, we have proposed a variable (s) description for the structural transition of the Mackay model between the 5-fold-symmetry icosahedral (ico) structure and the cuboctahedral (fcc) crystalline structure in clusters, and we have demonstrated, using ab initio molecular dynamics (MD) simulation, that, in Pb_{13}, the fcc-to-ico transition did follow this description. We have calculated the energy surface of the transition in Pb_{13}, which shows that the transition is barrierless. The atomic displacements of the structural transition in the fcc and ico Pb_{13} coincide with one of their vibrational eigenmodes with real and imaginary frequencies, respectively. The barriers of this transition path for Pb_n ($n = 55$, 147, and 309) were evaluated. The surprising oscillating behavior of the relative stability of ico and fcc Pb_n ($n = 13$, 55, 147, 309) clusters is quite different from the results obtained by various classical interatomic potentials. This fact strongly suggests that ab initio density functional theory (DFT) is needed in the study of nanosized clusters.

Acknowledgment. The authors gratefully acknowledge J. P. K. Doye for very helpful information. This work was supported by the National Science Council of Taiwan. The computer resources were mainly provided by the National Center for High-Performance Computing (HsinChu, Taiwan, ROC).

References and Notes

(1) (a) Farges, J.; de Feraudy, M. F.; Raoult, B.; Torchet, G. *J. Chem. Phys.* **1983**, *78*, 5067. (b) Farges, J.; de Feraudy, M. F.; Raoult, B.; Torchet, G. *J. Chem. Phys.* **1986**, *84*, 3491. (c) Farges, J.; de Feraudy, M. F.; Raoult, B.; Torchet, G. *Adv. Chem. Phys.* **1988**, *70*, 45.

(2) Koga, K.; Ikeshoji, T.; Sugawara, K. *Phys. Rev. Lett.* **2004**, *92*, 115507.

(3) Doye, J. P. K.; Calvo, F. *J. Chem. Phys.* **2002**, *116*, 8307.

(4) Hendy, S. C.; Hall, B. D. *Phys. Rev. B* **2001**, *64*, 85425.

(5) Mackay, A. L. *Acta Crystallogr.* **1962**, *15*, 916.

(6) For example, see http://chemistry.uoregon.edu/herrick.html.

(7) Mills, G.; Johsson, H.; Schenter, G. K. *Surf. Sci.* **1995**, *324*, 305.

(8) Hohenberg, P.; Kohn, W. *Phys. Rev.* **1964**, *136*, B864.

(9) Perdew, J. P.; Burke, K.; Ernzerhof, M. *Phys. Rev. Lett.* **1996**, *77*, 3865.

(10) Kohn, W.; Sham, L. J. *Phys. Rev.* **1965**, *140*, A1133.

(11) (a) Kresse, G.; Hafner, J. *Phys. Rev. B* **1993**, *47*, 558. (b) Kresse, G.; Hafner, J. *Phys. Rev. B* **1994**, *49*, 14251. (c) Kresse, G.; Furthmüller, J. *Phys. Rev. B* **1996**, *54*, 11169. (d) Kresse, G.; Furthmüller, J. *Comput. Mater. Sci.* **1996**, *6*, 15.

(12) Blöchl, P. E. *Phys. Rev. B* **1994**, *50*, 17953.

(13) Kresse, G.; Joubert, D. *Phys. Rev. B* **1999**, *59*, 1758.

(14) Sonntag, H.; Weber, R. *J. Mol. Spectrosc.* **1983**, *100*, 75.

(15) Frohen, F.; Schulze, W.; Kloss, U. *Chem. Phys. Lett.* **1983**, *99*, 500.

(16) Roos, B. O.; Malmqvist, P. *Phys. Chem. Chem. Phys.* **2004**, *6*, 2919 .

(17) Molina, L. M.; Lopez, M. J.; Rubio, A.; Balbas, L. C.; Alonso, J. A. *Adv. Quantum Chem.* **1999**, *33*, 329.

(18) Nosé, S. *J. Chem. Phys.* **1984**, *81*, 511.

(19) Uppenbrick, J.; David Wales, J. *J. Chem. Soc., Faraday Trans.* **1991**, *87*, 215.

(20) Doye, J. P. K. *Comput. Mater. Sci.* **2006**, *35*, 227.

(21) Rao, B. K.; Khanna, S. N.; Jena, P. *Phys. Rev. B* **2000**, *62*, 4666.

(22) Voter, A. F.; Chen, S. P. In *Characterization of Defects in Materials*; Siegel, R. W., Weertman, J. R., Sinclair, R., Eds.; MRS Symposia Proceedings No. 82; Materials Research Society: Pittsburgh, PA, 1987; p 175.